Solar Energy Materials & Solar Cells 93 (2009) 519–523

Contents lists available at ScienceDirect

Solar Energy Materials & Solar Cells

journal homepage: www.elsevier.com/locate/solmat

Optimizing hybrid photovoltaics through annealing and ligand choice

J.D. Olson, G.P. Gray, S.A. Carter *

Physics Department, University of California, Santa Cruz, CA 95064, USA

ARTICLE INFO

Article history:
Received 11 September 2008
Received in revised form
17 November 2008
Accepted 20 November 2008
Available online 18 January 2009

Keywords:
CdSe
P3HT
Photovoltaics
Polymer
Nanocrystal
Quantum dot

ABSTRACT

Photovoltaic devices made from blended cadmium selenide nanocrystals with various capping ligands and poly-3-hexylthiophene were prepared. The effects of capping ligands and annealing conditions were investigated. We find that capping ligands determine morphology/phase separation. Our findings suggest that annealing at temperatures between 105 and 122 °C yield optimized devices. We also report CdSe/P3HT blended devices with an efficiency of 1.8% under illumination by AM1.5D.

Published by Elsevier B.V.

1. Introduction

Third generation photovoltaics promise an affordable alternative to silicon-based technologies. By avoiding high-temperature processes, vacuum processes, and refined silicon, photovoltaics can be made much cheaper than conventional solar cells. If the materials are made wet-processable, solar cells can even be printed reel-to-reel. Polymer-based photovoltaics based on donor–acceptor heterojunctions offer an attractive pathway to low cost solar cells [1,2].

Polymer-based photovoltaics require two phases in the photoactive layer. These phases typically consist of fullerenes or nanocrystals for the acceptor phase, and polymers for the donor phase. Champion efficiencies for polymer–nanocrystal and polymer–fullerene single-junction cells are 2.8% [3] and 6.5% [4], respectively. These films are approaching efficiencies that would make a commercially viable technology, but more work must be done to improve efficiencies and improve device stability. While the degradation of polymer-based films has been subject of several studies [5,6], reproducible control over the phase separation between the donor and acceptor phases is also important to the viability of manufacturing high efficiency polymer-based solar cells.

In order to understand the impact of this phase separation on device performance, we blend poly(3-hexylthiophene-2,5-dyl) (P3HT) with cadmium selenide (CdSe) nanoparticles capped with various ligands and processed under different annealing conditions to understand the role that ligands have on determining blend morphology and ultimately the photovoltaic device performance. For nanocrystals to be soluble in traditional solvents, ligands are attached to the nanocrystal surface. Despite numerous studies showing distinction between CdSe nanoparticles capped with different ligands [7,9,10], few photovoltaic studies [11] have been done to determine what effects the various capping ligands have in the final device. The ligands often dominate the electrical performance of the nanocrystals since they can occupy electron surface states that otherwise would act as trap states for charge carriers [7] and can also act as insulators that impede charge transport. The ligands can also be a large driving force in nanocrystal aggregation [8] which can both improve charge transport and modify quantum confinement properties. We demonstrate that solution conditions, as well as ligand, can dramatically affect the blend morphology.

Thermal annealing is commonly employed in device processing and can strongly affect device performance. For polymer–fullerene devices, the enhancement is a result of enhanced phase separation and enhanced polymer crystallinity [12], but for P3HT/CdSe photovoltaics, the mechanism of performance enhancement is less clear. Contrary to previous results, our results suggest that improvements due to annealing are caused by oxygen removal rather than P3HT crystallization.

Under AM1.5G and 100 mW/cm^2, our best devices has yielded short circuit currents of 6.9 mA/cm^2, open circuit voltages of 0.55 V, and fill factors of 0.47 for a power conversion efficiency of 1.8%. This is not a record efficiency for the P3HT/CdSe system, but

* Corresponding author.
E-mail addresses: olson@physics.ucsc.edu (J.D. Olson), sacarter@ucsc.edu (S.A. Carter).

0927-0248/$ - see front matter Published by Elsevier B.V.
doi:10.1016/j.solmat.2008.11.022

it is the highest efficiency for CdSe nanodots, demonstrating that clever choice of ligands may prove a viable route to morphology control.

2. Experimental

Fig. 1(a) shows the energy structure for our devices; they are typical donor–acceptor photovoltaics. Absorption takes place in the nanocrystal/polymer phase, and excitons separate at the NC/polymer interface. By blending the phases, a large surface area is set up to aid this charge separation. Electrons preferentially remain in the NC and are extracted at the Al back electrode, while holes travel in P3HT to the ITO. These devices employ a poly(3,4-ethylenedioxythiophene) poly(styrenesulfonate) (PEDOT:PSS) electron-blocking layer, and holes are blocked from returning to the NC or aluminum contacts by a large offset between the donor HOMO and acceptor LUMO levels and contact fermi levels.

For this study, nanoparticles were synthesized by following the procedure given by Gur et al. [13]. Trioctylphosphine ligands were replaced with pyridine ligands by stirring the nanocrystals in an excess of pyridine under reflux for 24–48 h. If desired, a second ligand exchange was then performed using the same procedure with an excess of the replacement ligand. The capping ligands used were pyridine, butylamine, tributylamine, oleic acid, and stearic acid. The nanocrystals were then dispersed in chloroform, and mixed eight parts CdSe with one part of P3HT by weight. These mixtures were then diluted to 33 mg/ml of nanoparticles and stirred for at least 48 h. Devices were prepared on ITO coated glass substrates purchased from Thin Film Devices Inc. The substrates were cleaned by sonication in detergent at 60 °C, deionized water, and ethanol at 40 °C. They were then dried in a nitrogen stream. PEDOT:PSS was spin-cast onto the substrates at 3000 rpm and dried under vacuum at 110 °C for 1 h. Then CdSe nanoparticle/P3HT blend was spin-cast at various spin-speeds and dried for another hour under vacuum at 110 °C. Devices were then encapsulated in a nitrogen glove-box before evaporating 50 nm thick Al back-contacts.

Most of the nanoparticle/polymer blends were dispersed in pure chloroform, but some devices were made using a blended solvent of chloroform and capping ligand; this was done to control the aggregation of the nanoparticles. The capping ligand makes the nanoparticles soluble, and adding capping ligand to the solvent helps make them more so [8]. The polymer, however, is typically insoluble in the ligand, so a careful balance must be maintained to achieve proper dispersion. Therefore, concentrations of additional ligand were always kept below 5%.

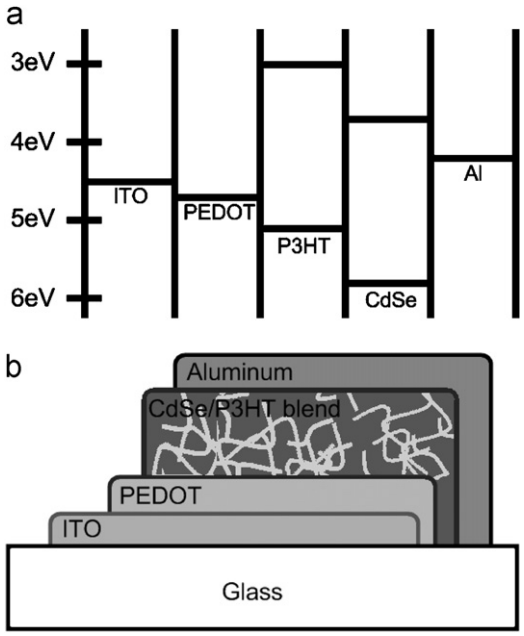

Fig. 1. Energy diagram and schematic of CdSe/P3HT blended devices.

$J-V$ characteristics were measured with a Keithley 2400 Sourcemeter under AM1.5D (100 mW/cm^2) simulated by an Oriel model 66902 solar simulator. The light intensity was calibrated using a NREL certified photodiode prior to each measurement. After initial testing, films were annealed for various times, typically at 100 °C for 30 min, and tested again. Unless otherwise noted, all figures depict devices after post-deposition annealing.

3. Results/discussion

While investigating an alternate ligand exchange procedure, Aldakov et al. noted that ligand choice affected phase separation [11]. We find the same here, and the level of phase separation dominated the behavior of these devices. Fig. 2 shows AFM images and $J-V$ characteristics of films prepared under identical conditions, but made from batches of nanocrystals capped with different capping ligands. The device short-circuit currents are almost completely explicable in terms of phase separation. Since the diffusion length is at most tens of nanometers, these devices will all be limited by their varying degrees of phase separation. Butylamine provides the best current and smallest morphology features, followed by oleic acid and tributylamine. Stearic acid devices have 10 μm scale structure, but finer structure on a scale of 500 nm exists across the morphology, partially explaining its relatively high performance. The only film not easily explained by phase separation was pyridine; films made with pyridine capped nanocrystals were consistently poor performers, with currents far lower than the phase separation would suggest. In fact, pyridine-capped films were much smoother than other blended films, suggesting a much lower phase separation, which may explain the low currents.

Nanoparticle synthesis has produced many geometries of nanoparticles, such as nanorods [14], tetrapods [15], and hyperbranched CdSe [16]. Photovoltaics based on these nanoparticles benefit from the varied geometries. CdSe nanorods have better charge transport than simple dots. Tetrapod and hyperbranched

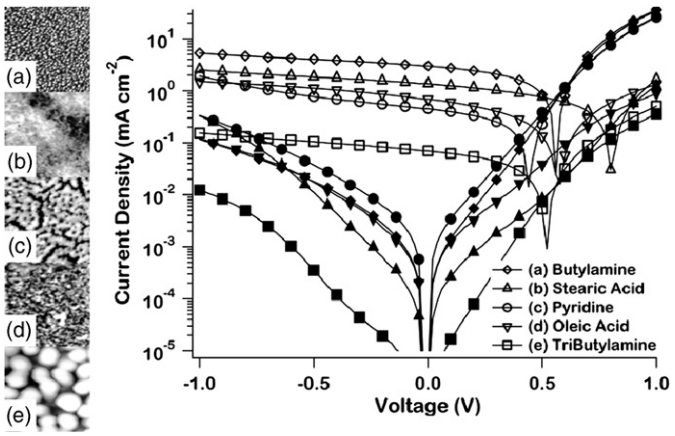

Fig. 2. AFM images and $J-V$ characteristics of NC/P3HT films identical in preparation except for the NC capping ligand. Ligands used were butylamine (a), stearic acid (b), oleic acid (c), pyridine (d), and tributylamine (e). Each AFM image is 15 μm^2. $J-V$ characteristics of post-production annealed devices. Light currents were recorded under a simulated AM1.5D spectrum at 100 mW/cm^2.

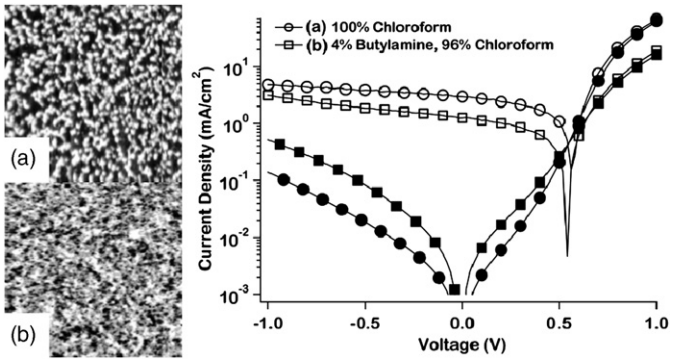

Fig. 3. AFM images and $J-V$ characteristics of CdSe/P3HT blended films. Films spun from solution containing no ligand (a) were rougher than films spun from solution with ligand (b). Light currents were recorded under a simulated AM1.5D spectrum at 100 mW/cm^2. AFM images are 15 microns square.

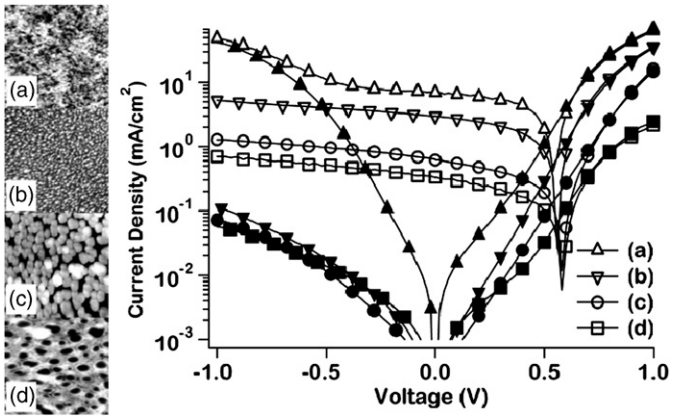

Fig. 4. $J-V$ characteristics and AFM images of devices made from various batches of butylamine-capped CdSe NCs. Filled shapes depict $J-V$ characteristics in the dark, and empty shapes show $J-V$ characteristics under simulated AM1.5D illumination. Each image is 15 μm^2.

nanocrystals may individually traverse the thickness of the film, and, at the very least, will have extensions perpendicular to the substrate, increasing the likelihood of a percolation pathway existing. This enhances performance by giving electrons a path to the photocathode. Top efficiencies for CdSe nanorods, tetrapods, and hyperbranched nanocrystals are 2.6% [14], 2.8% [3], and 2.2% [16], respectively. Our films benefit from a similar morphological advantage due to aggregation; since the aggregate size is often many times larger than the thickness of the film, these nanoparticle aggregates are likely to span the film in exactly the same manner. Some of the least aggregated of our films have average feature sizes larger than the film thickness (Fig. 3).

Previous works [8] used a tailored solvent to encourage less phase separation; adding capping ligand to the host solvent makes the nanoparticles more soluble at the expense of the polymer's solubility. This tailored solvent can decrease phase separation in the film. Our attempts to improve the morphology/phase separation in this manner were partially successful. These films became smoother, suggesting less phase separation, and the average feature size decreased, although evidence of aggregation was still present. Despite the improved morphology, photovoltaic performance decreased as the shunt resistance dropped (see Fig. 4). This is not likely due to additional ligand trapped in the film, as butylamine's boiling point is 25 °C below our processing temperature. More likely the original aggregation level was actually beneficial in this film by providing a percolation pathway in the same way a tetrapod-shaped nanocrystal would have.

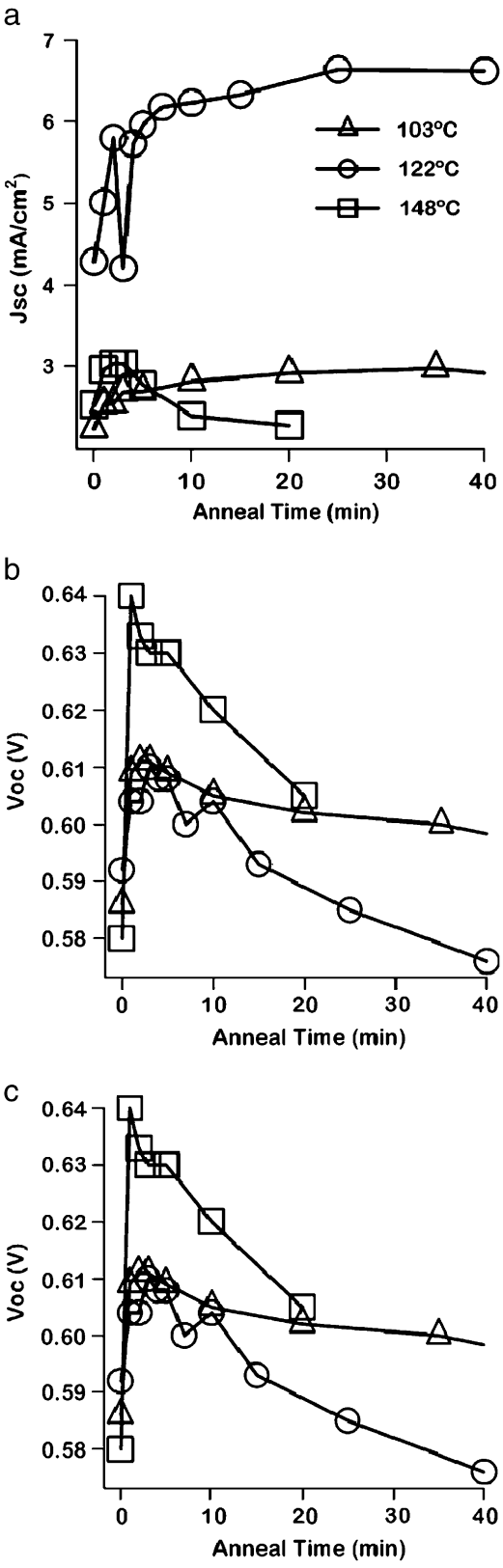

Fig. 5. Operating parameters are shown for butylamine-capped CdSe/P3HT devices as a function of anneal time. Samples were annealed at 103 °C (triangles), 122 °C (circles), and 148 °C (squares). This annealing was done after back-contact deposition in a nitrogen environment. Device parameters were recorded under AM1.5D at 100 mW/cm^2.

The pyridine-capped nanocrystals, which exhibited a similar level of aggregation, would likewise exhibit poor currents due to incomplete percolation pathways. A higher loading ratio of CdSe to P3HT may alleviate this problem.

Results can vary significantly between batches of nanoparticles, even with the same capping ligand. Each device in Fig. 4 was made from CdSe nanocrystals capped with butylamine. They were prepared under identical conditions, except for sample (a) [17]; the difference amongst these films is their parent batch of nanocrystals. A given batch of nanocrystals yielded similar film morphologies, but morphologies between batches varied significantly. This clearly suggests that differences in the nanoparticle solutions are responsible for these differences in morphology. The morphological differences result from differences in ligand exchange efficiency as noted by Sun et al. [15]. The cell performance correlates very well with the nanoparticle aggregation again.

Fig. 5 shows a summary of device photovoltaic parameters as a function of annealing for butylamine-capped NP devices. At all temperatures, the devices enjoyed a quick spike followed by a modest decline in open-circuit voltage. For the two lower temperatures, device parameters increased and stabilized over the course of 30 min, but parameters for devices annealed at 148 °C degenerated. Most notably, the fill-factor for these devices plummeted to less than 25% within 20 min.

Similar studies of annealing thin films of P3HT/PCBM have shown little difference in overall performance between films annealed once only either before or after back-contact deposition [18]. Although our samples are processed at 110 °C before back-contact deposition, they are subsequently exposed to oxygen, which quickly diffuses throughout the active layer [19]. Oxygen dissolved in the film would increase conductivity through the P3HT directly to the aluminum back contact, providing a shunt path [20]. Annealing removes this oxygen [21], so the improvement in parameters is expected.

Annealing at 105 and 122 °C serves mostly to remove oxygen from the P3HT, as can be seen in Fig. 6. The lower conductance, indicated by the lower currents in reverse bias, show fewer charge carriers as oxygen leaves the film [20]. However, as the temperature reaches 148 °C, the reverse bias conductance improves. The fill-factor for these films dropped with increasing reverse bias conductance. A similar behavior for ITO/PEDOT-PSS/P3HT/Au devices was observed by Chiguvare [22].

Superior butylamine-capped devices were made by changing the loading ratio to 12 parts to one of CdSe nanocrystal to P3HT. These devices were dispersed in chlorobenzene at a concentration of 60 mg/ml of CdSe. The resulting films were 130 nm thick. This procedure yielded devices with 0.55 Voc, 6.9 mA/cm^2 Jsc, and a

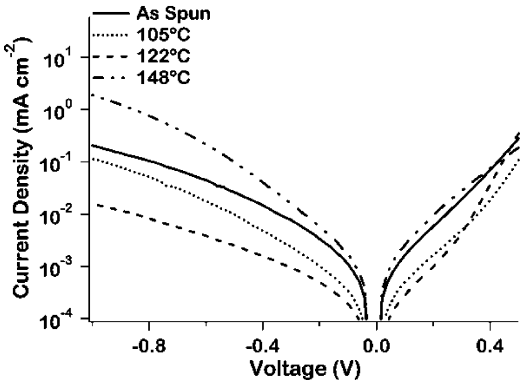

Fig. 6. $J-V$ characteristics of devices annealed for 20–25 min at different temperatures.

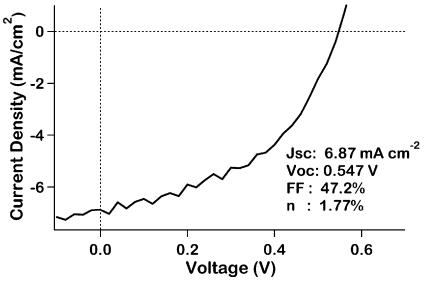

Fig. 7. $J-V$ characteristics of a superior butylamine-capped film. Light currents were recorded under a simulated AM1.5D spectrum at 100 mW/cm^2. This device displayed 1.8% power efficiency.

47% fill-factor. These 1.8% power efficient devices are the best reported to date on CdSe quantum-dot and P3HT blended films (see Fig. 7). We note that these devices have similar morphologies to optimum devices made from P3HT/CdSe nanorod blends. Furthermore, quantum dot and nanorod devices have very similar power efficiencies when chloroform is used as the solvent [14] which is known to result in less ordered polymer morphology. Quantum dots may have comparable efficiencies to quantum rod devices if a solvent with a higher boiling point was used to improve ordering and therefore hole transport within the polymer.

4. Conclusion

We have demonstrated that nanoparticle capping ligands, as well as solution conditions, have a dramatic effect on phase separation in blended nanocrystal/conjugated polymer devices. Optimal morphologies achieve a careful balance between the nanoparticle aggregation needed for good charge transport with phase separation needed for efficient exciton dissociation. Phase separation is heavily influenced by ligand choice, but inefficiencies in the ligand exchange procedure likely contribute to the final film morphology, as evidenced by the varied film morphologies resulting from films produced with different batches of nanocrystals under otherwise identical conditions. A thermal annealing step at around 110 °C after isolation from atmospheric conditions is critical to remove oxygen from the P3HT. As has been suggested by other recent work [23], new methods to control the phase separation dynamics in polymer–nanoparticle blends will be important to the future viability of this technology.

Acknowledgments

The authors thank the University of California Discovery program for support, and Dr. Damoder Reddy and Dr. Yudhisthira Sahoo for providing CdSe nanocrystals.

References

[1] B.R. Saunders, M.L. Turner, Nanoparticle–polymer photovoltaic cells, Adv. Colloid Interface Sci. 138 (2008) 1–23.
[2] B.C. Thompson, J.M.J. Fréchet, Polymer–fullerene composite solar cells, Angew. Chem. Int. Ed. 47 (2008) 58–77.
[3] B. Sun, H.J. Snaith, A.S. Dhoot, S. Westenhoff, N.C. Greenham, Vertically segregated hybrid blends for photovoltaic devices with improved efficiency, J. Appl. Phys. 97 (2005) 014914.
[4] J.Y. Kim, K. Lee, N.E. Coates, D. Moses, T. Nguyen, M. Dante, A.J. Heeger, Efficient tandem polymer solar cells fabricated by all-solution processing, Science 317 (2007) 222–225.
[5] M. Jørgensen, K. Norrman, F.C. Krebs, Stability/degradation of polymer solar cells, Sol. Energy Mater. Sol. Cells 92 (2008) 686–714.

[6] J.A. Hauch, P. Schilinsky, S.A. Choulis, R. Childers, M. Biele, C.J. Brabec, Flexible organic P3HT:PCBM bulk-heterojunction modules with more than 1 year outdoor lifetime, Sol. Energy Mater. Sol. Cells 92 (2008) 727–731.
[7] G. Kalyuzhny, R.W. Murray, Ligand effects on optical properties of CdSe nanocrystals, J. Phys. Chem. B 109 (2005) 7012–7021.
[8] W.U. Huynh, J.J. Dittmer, W.C. Libby, G.L. Whiting, A.P. Alivisatos, Controlling the morphology of nanocrystal–polymer composites for solar cells, Adv. Funct. Mater. 13 (2003) 73–79.
[9] M. Kuno, J.K. Lee, B.O. Dabbousi, F.V. Mikulec, M.G. Bawendi, The band edge luminescence of surface modified nanocrystallites: probing the luminescing state, J. Chem. Phys. 106 (1997) 9869–9882.
[10] C. Querner, P. Reiss, S. Sadki, M. Zagorska, A. Pron, Size and ligand effects on the electrochemical and spectroelectrochemical responses of CdSe nanocrystals, Phys. Chem. Chem. Phys. 7 (2005) 3204–3209.
[11] D. Aldakov, F. Chandezon, R.D. Bettignies, M. Firon, P. Reiss, A. Pron, Hybrid organic–inorganic nanomaterials: ligand effects, Eur. Phys. J. Appl. Phys. 36 (2006) 261–265.
[12] M. Reyes-Reyes, K. Kim, D.L. Carroll, High-efficiency photovoltaic devices based on annealed poly(3-hexylthiophene) and 1-(3-methoxycarbonyl)-propyl-1-phenyl-(6,6)C_{61} blends, Appl. Phys. Lett. 87 (2005) 083506.
[13] I. Gur, N.A. Fromer, M.L. Geier, A.P. Alivisatos, Air-stable all-inorganic nanocrystal solar cells processed from solution, Science 310 (2005) 462–465.
[14] B. Sun, N.C. Greenham, Improved efficiency of photovoltaics based on CdSe nanorods and poly(3-hexylthiophene) nanofibers, Phys. Chem. Chem. Phys. 8 (2006) 3557–3560.
[15] B. Sun, E. Marx, N.C. Greenham, Photovoltaic devices using blends of branched CdSe nanoparticles and conjugated polymers, Nano Lett. 3 (2003) 961–963.
[16] I. Gur, N.A. Fromer, C. Chen, A.G. Kanaras, A.P. Alivisatos, Hybrid solar cells with prescribed nanoscale morphologies based on hyperbranched semiconductor nanocrystals, Nano Lett. 7 (2007) 409–414.
[17] This sample was prepared at a higher loading ratio (27:2) and at a higher concentration (74.5 mg/ml).
[18] G. Li, V. Shrotriya, Y. Yao, Y. Yang, Investigation of annealing effects and film thickness dependence of polymer solar cells based on poly(3-hexylthiophene), J. Appl. Phys. 98 (2005) 043704.
[19] L. Lüer, H.J. Egelhaaf, D. Oelkrug, G. Cerullo, G. Lanzani, B.H. Huisman, D. de Leeuw, Oxygen-induced quenching of photoexcited states in polythiophene films, Org. Electron. 5 (2004) 83–89.
[20] M.S.A. Abdou, F.P. Orfino, Y. Son, S. Holdcroft, Interaction of oxygen and conjugated polymers: charge transfer complex formation with poly (3-alkylthiophenes), J. Am. Chem. Soc. 119 (1997) 4518–4524.
[21] B.A. Mattis, P.C. Chang, V. Subramanian, Effect of thermal cycling on performance of poly(3-hexylthiophene) transistors, Mater. Res. Soc. Symp. Proc. 771 (2003) L10.35.
[22] Z. Chiguvare, Electrical and optical characterisation of bulk heterojunction polymer–fullerene solar cells, Ph.D. Thesis, Oldenburg University, Oldenburg, Germany, 2005.
[23] I. Gur, N.A. Fromer, C. Chen, A.G. Kanaras, A.P. Alivisatos, Hybrid solar cells with prescribed nanoscale morphologies based on hyperbranched semiconductor nanocrystals, Nano Lett. 7 (2007) 409–414.